

# PREDICTIVE MODELLING OF AVIRIS PERFORMANCE OVER INLAND WATERS

Dekker, A.G. and Hoogenboom, H.J.

Institute for Environmental Studies, De Boelelaan 1115, 1081 HV Amsterdam, The Netherlands.

Tel 31-20-4449506; Fax 31-20-4449553; email: arnold.dekker@ivm.vu.nl.

## 1. INTRODUCTION

The availability of imaging spectrometers such as AVIRIS, CASI, ROSIS, HYDICE etc. has created a necessity for spectral methods and models which can predict the performance of these instruments for detecting and estimating a certain parameter, e.g. chlorophyll  $\alpha$  as a water quality indicator. The method presented here predicts which wavelength bands are best suited for estimating a parameter quantitatively and uniquely. Based on a model relating the specific inherent optical properties (IOP) to the subsurface reflectance,  $R(0^-)$  over eutrophic lake waters, simulations of the effects of concentration ranges of chlorophyll  $\alpha$  to the reflectance were performed. The other optically active constituents such as aquatic humus, seston dry weight, or the non-phytoplankton part of the seston could be varied also. Using the noise-equivalent-radiance values for AVIRIS the performance of AVIRIS for detecting chlorophyll  $\alpha$  could be calculated. By using such a predictive method costly measurement campaigns, involving field and laboratory work, with possible disappointing results may be avoided.

Before describing the model it is useful to point out three different approaches by which measurements of spectral (ir)radiance can be used to estimate concentrations of water constituents in remote sensing. Based on Morel and Gordon (1980) two approaches establish statistical relationships: i.e. the empirical and the semi-empirical approach; whereby the semi-empirical method includes spectral knowledge in the analysis. The third, analytical approach is based on physical modelling and is therefore preferred. Gordon & Morel (1983) give a comprehensive discussion of the analytical models available for clear ocean waters through to turbid coastal waters. Kirk (1983, 1994) and Dekker et al (1994) extended the discussion to inland waters. In the analytical models inherent and apparent optical properties of the water constituents are used to model the reflectance and vice versa. The water constituents are expressed in their specific (per unit measure) absorption and backscatter coefficients. Subsequently, a suite of analysis methods can be used to optimally retrieve the water constituents or water quality parameters from the remotely sensed upwelling radiance or radiance reflectance signal.

Dekker (1993) developed remote sensing algorithms following the analytical approach for estimation of both *in situ* chlorophyll  $\alpha$  and cyanophycocyanin concentrations from airborne remotely sensed radiance measurements, calibrated to subsurface irradiance reflectance  $R(0^-)$ . This approach required the estimation of specific absorption and backscattering coefficients for both algal and non-algal particulate matter. The chlorophyll  $\alpha$  algorithms were determined from spectrophotometric measurements of apparent absorption and scattering. Chlorophyll  $\alpha$  could be derived from the actual airborne remote sensing radiance with an accuracy of  $9.5 \text{ mg m}^{-3}$  and cyanophycocyanin with an accuracy of approximately  $20 \text{ mg m}^{-3}$ . These algorithms were developed using only two bands with centres at 676 and 706 nm respectively and a bandwidth of 10 nm wide. This was required because the two airborne scanners used had a limited amount of spectral bands available: The Netherlands CAESAR has nine spectral bands in the Inland Water Mode (using filters) and the CASI had (in 1990 and 1993) 15 programmable spectral bands available in the spatial mode. In order to compare the CASI data with the CAESAR data the bands were kept similar. CASI does allow a selection of 15 bands over the range of 430 to 870 nm.

However, AVIRIS has different wavelength centres, bandwidths and signal-to-noise ratios. Furthermore, AVIRIS measures the optical and nearby and middle infrared spectrum continuously, so a selection of bands is not *a priori* necessary. Thus in order to gain insight into the performance of AVIRIS a spectral model was constructed

that enabled the determination of the effect of increasing chlorophyll  $\alpha$  on the spectral  $R(0-)$ . A subsequent translation of  $R(0-)$  to the noise equivalent radiance difference as measured by AVIRIS (without atmospheric influence!), gives a indication of the accuracy for AVIRIS in estimating chlorophyll  $\alpha$ .

## 2. METHOD

The method used in this study contains five steps:

- parameterisation of the bio-optical model
- run bio-optical model for a range of values for the water constituents, especially CHL
- obtain resolvability of  $R(0-)$  by calculating the derivative of  $R(0-)$  with respect to CHL
- convert  $R(0-)$  to upwelling radiance above the air-water interface
- compare the radiance with noise equivalent radiance of AVIRIS (1995)

Before discussing the method and the model a series of subsurface reflectance spectra ( $R(0-)$ ) measured in a variety of inland waters of widely differing trophic status in the Netherlands is presented and discussed. From these measurements two representative water types were selected: i.e. shallow eutrophic lakes and deep lakes. The  $R(0-)$  measurements enable validation of the results of the model. The spectra are presented in Fig. 1. The chlorophyll  $\alpha$  values ranged from 25  $\text{mg m}^{-3}$  to 120  $\text{mg m}^{-3}$  CHL. Reflectance in these water bodies is low in the blue end of the spectrum (400-500 nm) as a result of relatively high concentrations of aquatic humus (=dissolved yellow substance) in nearly all Dutch waters. With increasing wavelength reflectance is markedly affected by particulate matter. Lakes with relatively low phytoplankton and suspended matter concentrations have low reflectance, water bodies with low phytoplankton but high suspended matter concentrations have high reflectance up to 720 nm, and lakes with high phytoplankton and suspended matter concentrations have a similarly high reflectance but punctuated by absorption features due to photosynthetic pigments in phytoplankton. The additional effects of particulate backscattering and humic absorption in inland waters introduce complex interacting relations between the water constituents and subsurface reflectance. From these observations qualitative conclusions can be drawn on the effect of constituent concentration on  $R(0-)$  at different wavelengths. By using a bio-optical model a more quantitative analysis becomes feasible.

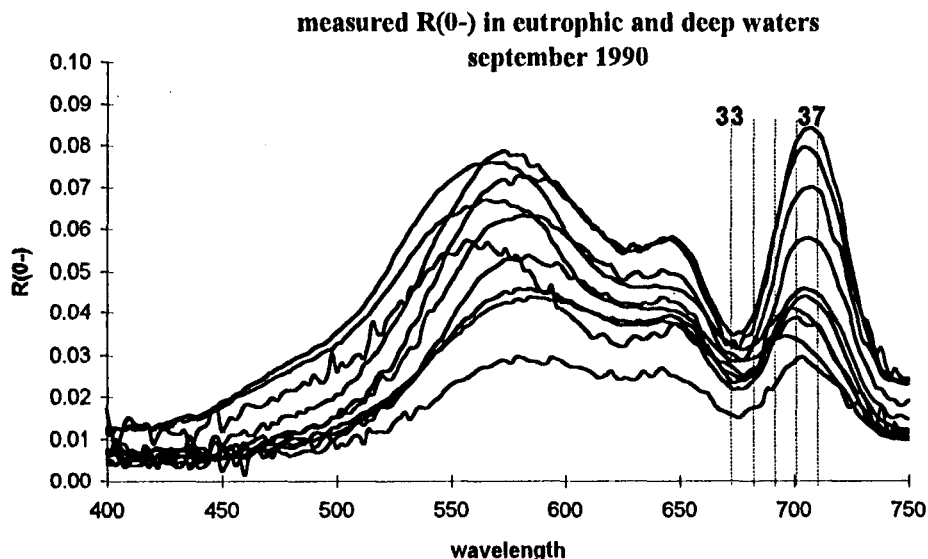


Figure 1. Measured  $R(0-)$  representative for shallow eutrophic and deep inland waters with CHL values ranging from 25 to 120  $\text{mg m}^{-3}$ . The dotted lines are the centre wavelengths of AVIRIS channels 33 to 37.

### 3. A BIO-OPTICAL MODEL FOR INLAND WATERS

#### 3.1 The relation between $R(0-)$ and water constituent concentrations in inland waters

The underwater light field is determined by the inherent optical properties (IOP) which are independent of the ambient light field (i.e. independent of changes in the angular distribution of radiant flux). Within the scope of this study these properties are specified by the absorption coefficient  $a$  ( $m^{-1}$ ) and the backscattering coefficient  $b_b$  ( $m^{-1}$ ). In inland waters the spectral reflectance is predominantly a function of: (i) absorption by algal pigments, aquatic humus and tripton (the non-phytoplankton part of the suspended matter) at short wavelengths and by pure water at longer wavelengths, (ii) (back)scattering by phytoplankton and tripton which can be up to 1000 times the backscattering of oceanic waters.

The relation between  $R(0-)$  and the inherent optical properties (IOP) for ocean and inland waters systems was investigated by (Gordon *et al.*, 1975, Morel and Prieur, 1977; Whitlock *et al.*, 1981 ; Kirk, 1991; Dekker, 1993; Dekker *et al.*, 1994). Dekker *et al.*, 1994, found that the following linear backscattering albedo model was the most appropriate model for inland waters:

$$R(0-) = r_1 \frac{b_b(\lambda)}{a(\lambda) + b_b(\lambda)}, \quad \text{eq. 1}$$

Values of  $r_1$  ranged from 0.12 to 0.56 and appeared to be lake-specific. The IOP of all four optically active components are included in the model and are denoted by their first character: phytoplankton (p), tripton (t), aquatic humus (h) and water (w).

#### 3.2 The inherent optical properties: parametrization of the bio-optical model

The model is used to simulate the effect of changes in chlorophyll  $\alpha$  (CHL) concentration on  $R(0-)$ . It is necessary to select appropriate values for each of the specific inherent optical properties, i.e. the inherent optical properties per unit water quality parameter: e.g. the specific inherent absorption by chlorophyll  $\alpha$ ,  $a_p^*$ , is the amount of absorption caused by  $1 \mu g l^{-1}$  chlorophyll  $\alpha$ .

$$a = a_p^* CHL + a_t^* C_t + a_h^* a_h(440) + a_w \quad \text{eq. 2}$$

$$b_b = b_{bp}^* CHL + b_{bt}^* C_t + b_{bw} = b_{bs}^* \{CHL + C_t\} + b_{bw}$$

Specific IOP are denoted by an asterix as superscript. Values for the IOP in this model are:

$a_w$ : The temperature dependent absorption by pure water from Buiteveld *et al.* (1994)

$b_{bw}$ : The backscattering of pure water from Buiteveld *et al.* (1994)

$a_p^*$ : specific inherent absorption by chlorophyll  $\alpha$  derived from Dekker (1993)

$a_t^*$ : specific inherent absorption by tripton from Dekker (1993). The concentration of tripton  $C_t$  in  $mg l^{-1}$  cannot be determined directly but was calculated by subtracting the algal fraction of seston dry weight from the total seston dry weight (DW). The algal fraction of seston dry weight was estimated using an empirical relation  $DW(p) = 0.07 CHL$  (Buiteveld, 1995). The tripton absorption was divided by the tripton dry weight yielding the specific inherent tripton absorption.

$b_{bs}^*$ : specific inherent backscattering of seston (i.e. the sum of tripton and phytoplankton): although it would be preferable to have a separate specific inherent backscattering for tripton and phytoplankton this is not available currently.

$a_h^*$ : the specific absorption coefficient of aquatic humus is calculated by assuming an exponential slope for aquatic humus absorption and taking the absorption by aquatic humus at 440 nm  $a_h(440)$  (g440 as defined by Kirk (1994) as a measure of the aquatic humus concentration (c.f. eq. 2):

$$a_h^*(\lambda) = e^{S(\lambda-440)} \quad \text{eq. 3}$$

This equation is based on the assumption of a fixed slope, where  $S$  is stated to be independent of the choice of reference wavelength. An analysis of the  $a_h^*$  values obtained between 400 - 800 nm for water bodies in this study showed a correspondence to an exponential function with an average value of  $S = 0.0146 \text{ nm}^{-1}$  (Dekker, 1993).

In natural inland waters there is often a significant correlation between chlorophyll  $\alpha$  and both aquatic humus and tripton concentrations. Therefore, increases in chlorophyll  $\alpha$  in the model (first series) are associated with, in nature, occurring increases in aquatic humus and tripton. Using linear regression for nine samples in the shallow eutrophic lakes, the following equations were derived:

$$\begin{aligned} a_h(440) &= 1.78 + 0.009 * CHL & r^2 &= 0.69 \\ C_t &= 11.54 + 0.042 * CHL & r^2 &= 0.74 \end{aligned} \quad \text{eq. 4}$$

### 3.3 Resolvability with respect to CHL

The derivative of  $R(0-)$  with respect to CHL can be considered as a measure of the resolvability of  $R(0-)$  due to changes in CHL. The change in  $R(0-)$ ,  $\Delta R(0-)$ , due to a user defined accuracy in CHL,  $\Delta CHL$ , is approximately

$$\Delta R(0-) = \frac{\partial R(0-)}{\partial CHL} \Delta CHL \quad \text{eq. 5}$$

This means that the sensitivity of the instrument should be sufficient to detect these changes in  $R(0-)$ . The (partial) derivative of  $R(0-)$  with respect to CHL can be found from eq. 2, yielding

$$\frac{\partial R(0-)}{\partial CHL} = r_1 \frac{b_{br}^* a_r - a_p^* b_{br}}{\left[ a_r + b_{br} + (a_p^* + b_{br}^*) CHL \right]^2} \quad \text{eq. 6}$$

From inspection of eq. 6 we can draw some qualitative conclusions:

- in terms of the effect on  $R(0-)$  there is a balancing effect between the backscattering and the absorption of phytoplankton;
- the sensitivity of  $R(0-)$  due to changes in CHL decreases for increasing values of CHL.

The derivative of  $R(0-)$  can not directly be compared with the sensitivity of AVIRIS, but has to be converted to a radiance above the air-water interface as measured by AVIRIS. Using a simplified air-water interface correction (Dekker, 1993) the following expression for the derivative of the above surface upwelling radiance with respect to CHL can be derived:

$$\frac{\partial I_{au}}{\partial CHL} \approx \frac{I_0}{2.89} \frac{\partial R(0-)}{\partial CHL}, \quad \text{eq. 7}$$

where  $I_0$  is a panel-based downwelling radiance measurement. Eq. 7 expresses the change in upwelling radiance due to a change of  $1 \text{ mg m}^{-3}$  of CHL (note that this change depends on the CHL already present (c.f. eq. 6)). The absolute values of the changes in radiance can be compared with the noise equivalent radiance of AVIRIS, indicating the performance of AVIRIS for detecting changes in CHL.

## 4. RESULTS

### 4.1 Simulations for shallow eutrophic lakes

In the first series of simulations, correlations between the organic compounds were introduced as given above (eq.4) in order to represent natural conditions in shallow eutrophic lakes. Figure 2a and b show the results for  $R(0-)$  and the derivative of  $R(0-)$  to chlorophyll  $\alpha$ . In this simulation the effect of increasing chlorophyll  $\alpha$  concentrations is given in increments of  $20 \text{ mg m}^{-3}$  ranging from  $20$  to  $200 \text{ mg m}^{-3}$ . The aquatic humus and tripton concentrations increase linearly according to eq. 4.

The results indicate that at  $400 \text{ nm}$  there is a hinge point where the  $R(0-)$  does not change : the increase in absorption by phytoplankton, tripton and aquatic humus is balanced by the increase in scattering of the phytoplankton and tripton. From  $410$  to  $660 \text{ nm}$  there is a decrease in reflectance within the same order of magnitude over this wavelength range, but it becomes exponentially less as the concentration of chlorophyll  $\alpha$  increases. In the spectral area between  $660$  and  $720 \text{ nm}$   $R(0-)$  changes more. Fig 2a and b both show that the decrease in  $R(0-)$  at  $676$  and  $750 \text{ nm}$  is constant for all CHL. The maximum of  $R(0-)$  initially at  $696 \text{ nm}$  for  $\text{CHL}=20 \text{ mg m}^{-3}$  shifts to a maximum at  $710 \text{ nm}$  for  $\text{CHL}=200 \text{ mg m}^{-3}$ . Thus for AVIRIS the channel 34 centered at  $674 \text{ nm}$  in combination with channels 36 to 38 are required in order to detect such a range in these type of waters, provided a ratio algorithm is to be used. In fact, channel 36 is most suited for ranges up to  $20 \text{ mg m}^{-3}$  channel 37 for ranges in CHL of  $40$  to  $120 \text{ mg m}^{-3}$  and channel 38 for concentrations from  $120$  to  $200 \text{ mg m}^{-3}$ . The derivative of  $R(0-)$  in Fig. 2b shows even clearer which wavelengths are suited to discriminate reflectance differences caused by the changes in chlorophyll  $\alpha$ . Most interesting however is the stable point at  $696 \text{ nm}$  which might be a potentially important spectral location for developing new algorithms.

### 4.2 Simulations for deep lakes (with algae bloom)

In the second series of simulations the concentrations of the phytoplankton, tripton and aquatic humus were assumed to be uncorrelated. In order to model a bloom occurring in a deep lake the  $a_h(440)$  and  $C_t$  were fixed at specific values of  $0.5 \text{ m}^{-1}$  and  $1 \text{ mg l}^{-1}$  respectively. This may be seen as a model of a bloom occurring under maximal growth conditions for the algae with no extra detritus being created during the increase in chlorophyll  $\alpha$ . Figure 3a and b show the results for  $R(0-)$  and the derivative of  $R(0-)$  to chlorophyll  $\alpha$ .

The resulting  $R(0-)$  spectra (Fig. 3a) are significantly different from series 1 (Fig. 2a). There is a range from  $400$  to  $530$  with some change in  $R(0-)$ . In the derivative (Fig. 3b) there are two hinge points: at  $420$  and at  $530 \text{ nm}$ . This may be a similar phenomenon that causes the blue-to-green ratio often used for ocean waters to work. In this case it seems that a blue to green ratio with a band below  $420$  and a band around  $480 \text{ nm}$  would discriminate up to  $60 \text{ mg m}^{-3}$  CHL. From  $530$  to  $650 \text{ nm}$   $R(0-)$  increases in the same order of magnitude with increasing CHL (note that in series 1 there was a decrease of  $R(0-)$  in this spectral region). At  $676 \text{ nm}$  the  $R(0-)$  is stable with increasing CHL: this points to a counter balance between the increase in absorption and the increase in backscattering by the phytoplankton. The increase in  $R(0-)$  at the  $700 \text{ nm}$  area is the most discriminative of the entire spectrum; especially for concentrations over  $60 \text{ mg m}^{-3}$  CHL (as compared to anywhere from  $530$  to  $650 \text{ nm}$ ). Once again it appears that a ratio algorithm involving the  $674 \text{ nm}$  spectral band and the  $696$  to  $710 \text{ nm}$  range is most suited for estimating CHL in a range from  $20$  to  $200 \text{ mg m}^{-3}$  CHL. The increase in  $R(0-)$  beyond  $710 \text{ nm}$  through to  $750 \text{ nm}$  is also remarkable and a clear indication that this nearby infrared region is worth investigating further: e.g. the increase in  $R(0-)$  at  $750 \text{ nm}$  is solely due to the increase in backscattering caused by the phytoplankton. As for the first series the derivative spectrum shows a stable increase of  $R(0-)$  at  $750 \text{ nm}$  with increasing CHL. A spectral band in the area of  $710$  to  $750 \text{ nm}$  may thus serve as a reliable indicator of changing backscattering in a lake.

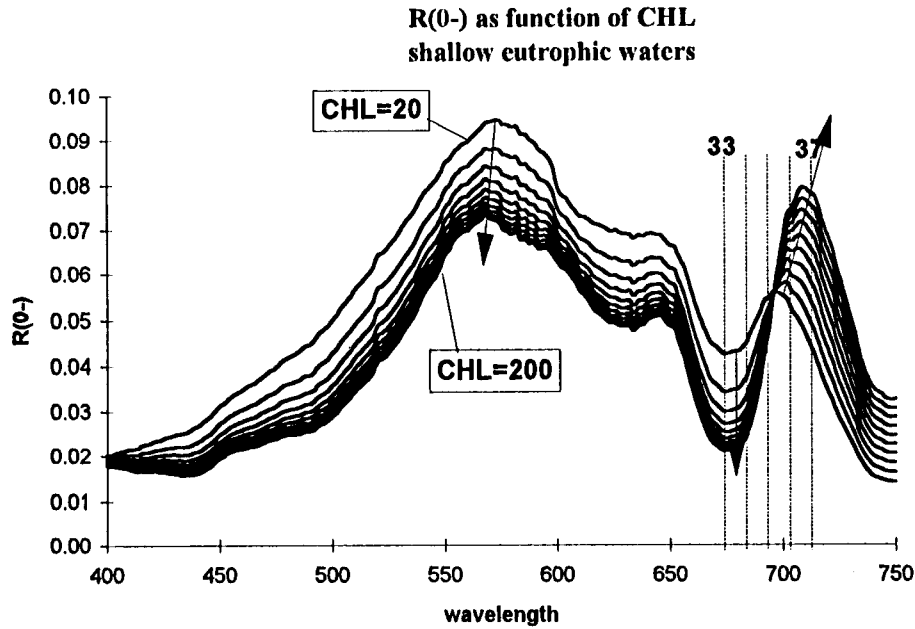


Figure 2a. Modelled  $R(0-)$  as a function of increasing CHL with associated increases in tripton and aquatic humus. The CHL ranges from 20 to 200  $\text{mg m}^{-3}$  with increments of 20  $\text{mg m}^{-3}$ . The dotted lines are the centre wavelengths of the AVIRIS channels 33- 37.

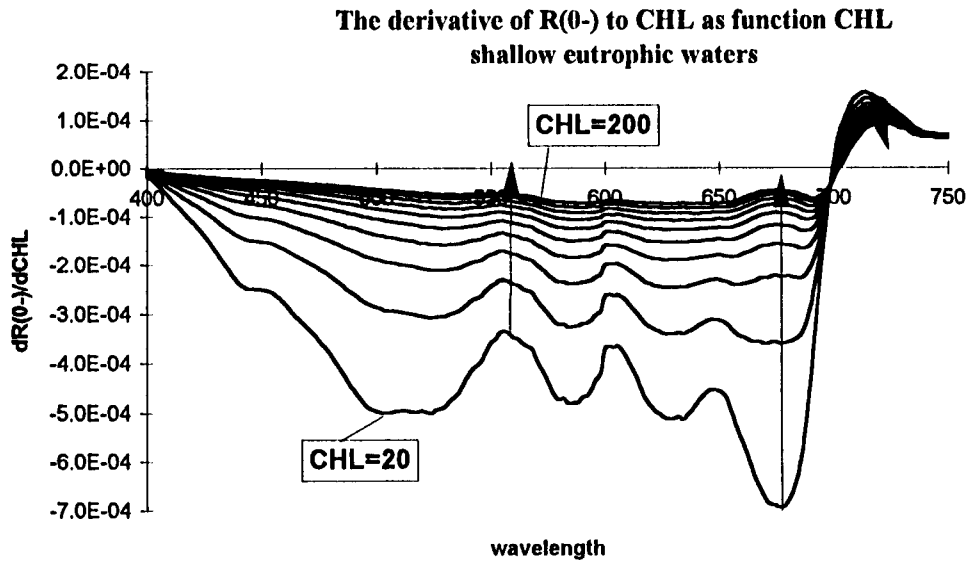


Figure 2b. The derivative of  $R(0-)$  to CHL as a function of CHL. The same data as in Fig. 2a are used.

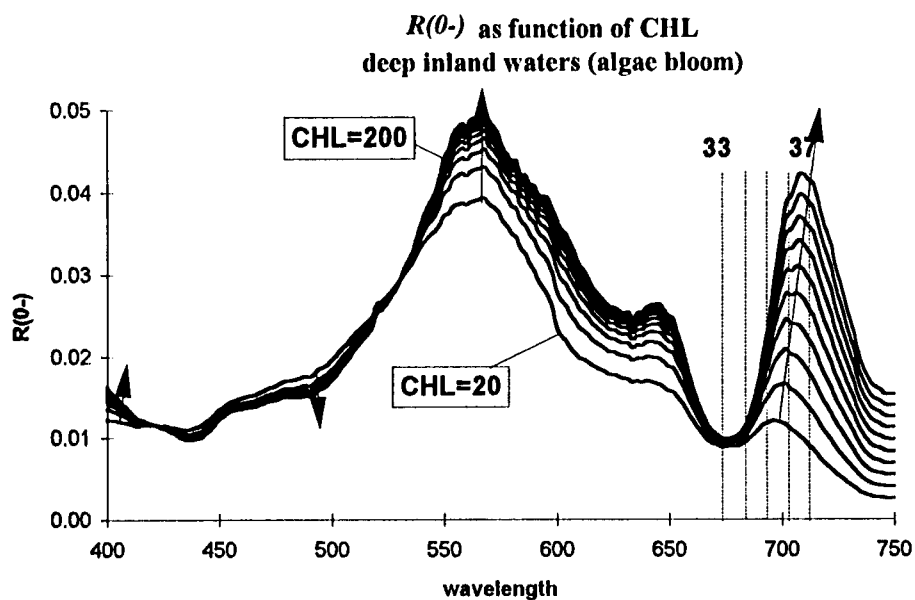


Figure 3a. Modelled  $R(0-)$  as a function of increasing CHL levels with fixed values for tripton and aquatic humus. The CHL ranges from 20 to 200  $\text{mg m}^{-3}$  with increments of 20  $\text{mg m}^{-3}$ . The dotted lines are the centre wavelengths of the AVIRIS channels 33- 37.

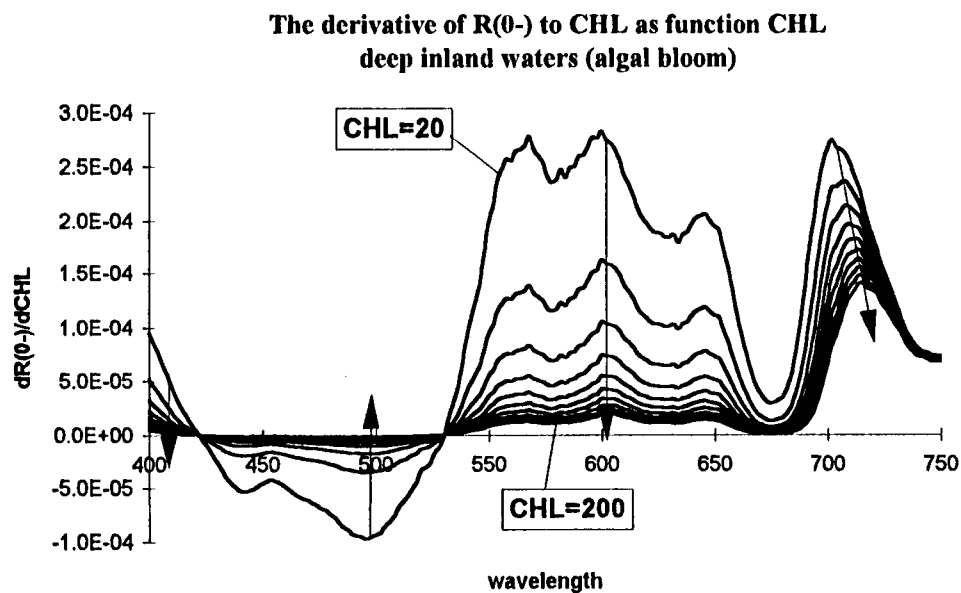


Figure 3b. The derivative of  $R(0-)$  to CHL as a function of CHL. The same data as in Fig. 3a are used.

### 4.3 An estimation of the accuracy with which AVIRIS may estimate chlorophyll $\alpha$ in eutrophic lakes.

Based on the first series of simulations an estimate was made for the accuracy with which AVIRIS may detect CHL levels in inland waters. A downwelling radiance as was calculated for a solar zenith angle of  $30^\circ$ , a horizontal visibility of 10 km was entered into eq. 7 and absolute values of the derivative of  $L_{au}$  were calculated, see Fig 4. The noise equivalent radiance (NEDL) of AVIRIS(1995) is also given in Fig. 4 (the dashes) and from the comparison it shows that at low concentrations of CHL =  $20 \text{ mg m}^{-3}$  AVIRIS can discriminate differences of  $2.8 \text{ mg m}^{-3}$  at 674 nm (CH 34). However, with increasing CHL this resolving power reduces to  $42 \text{ mg m}^{-3}$  at  $200 \text{ mg m}^{-3}$  at 676 nm. If, however, a ratio of the 674 to e.g. a 713 band (CH 38) is used for estimating CHL these figures will improve. Especially for the higher concentrations of CHL, because the derivative of  $L_{au}$  to CHL is in the order of  $22 \text{ mg m}^{-3}$  over the  $20 - 200 \text{ mg m}^{-3}$  range at 700 to 720 nm. This accuracy is, in general, sufficient for inland water management purposes. Of course, during an actual flight of AVIRIS, the atmospheric and air-water interface effects may add considerable noise and reduce the accuracy of the signal, thereby reducing AVIRIS's effective resolving power.

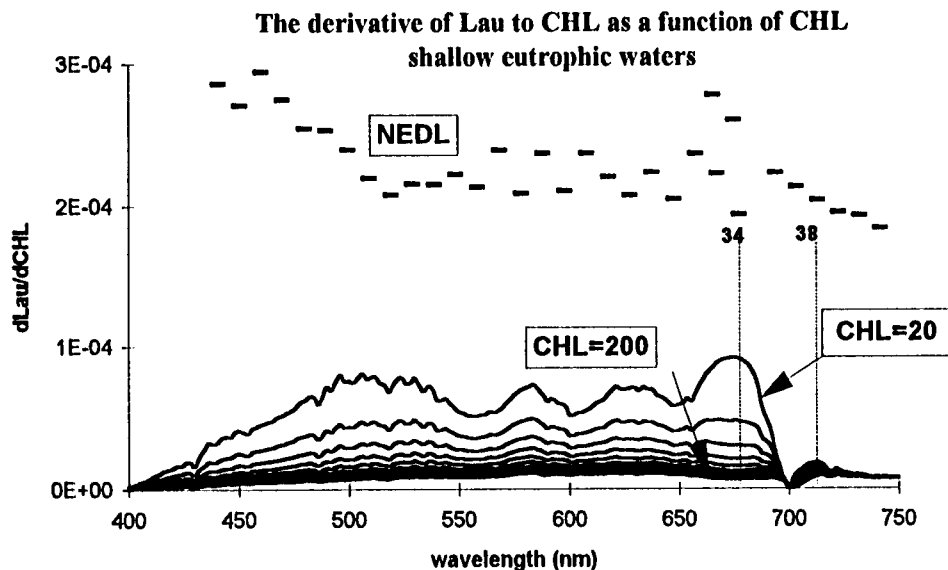


Figure 4. The derivative of the upwelling radiance  $L_{au}$  with respect to CHL for a range of CHL levels from 20 to  $200 \text{ mg m}^{-3}$  with increments of  $20 \text{ mg m}^{-3}$ . The NEDL of AVIRIS is denoted by the dashes. The graph should be read as follows: At a concentration of CHL =  $20 \text{ mg m}^{-3}$  the line  $dL_{au}/dCHL$  represents the NEDL required to discriminate a CHL concentration difference of  $1 \text{ mg m}^{-3}$ .



## 5. CONCLUSIONS AND DISCUSSION

A predictive model for estimating the effect of varying concentrations of a water quality parameter on the reflectance signal from a waterbody is a powerful tool in assessing the potential of remote sensing instruments such as AVIRIS. These models may also play an important role in defining preset spectral bands for instruments such as the CASI or the (planned) ESA satellite imaging spectrometer MERIS or for MODIS. Another important role for such models is for developing robust algorithms for detecting chlorophyll  $\alpha$  or any other optical water quality parameter. Especially the capability to simulate co-varying, or independently varying optical water quality parameters is a valuable asset and pushes the development of algorithms beyond the scope offered by the empirical or semi-empirical approach.

Two simulation series, assuming increases of CHL in steps of  $20 \text{ mg m}^{-3}$  from  $20 \text{ mg m}^{-3}$  to  $200 \text{ mg m}^{-3}$ , one with covarying concentrations of aquatic humus and tripton and one with stable concentrations of aquatic humus and tripton, showed significant influence on the size and shape of the  $R(0-)$  spectra and the derivative spectra of  $R(0-)$  to CHL. In fact several hinge points in the  $R(0-)$  were identified, that indicate spectral areas where increases in absorption are compensated by increases in backscattering. It was also possible to identify areas in the derivative spectra where the rate of change of  $R(0-)$  with increasing CHL levels was either exponential or linear. A preliminary comparison with actual *in situ* measured spectra showed a good comparison with the modelled spectra. If a ratio algorithm for chlorophyll were to be used of the form  $R(0-)_{676}/R(0-)_{700}$ , it has become obvious from this modeling exercise that several adjacent bands of AVIRIS are required in order to monitor the shift in the nearby infrared reflectance: the peak shifts from 696 at  $20 \text{ mg m}^{-3}$  to 710 nm at  $200 \text{ mg m}^{-3}$  CHL, requiring the use of AVIRIS channels 36, 37 and 38. Another important conclusion drawn from the modelling results is that AVIRIS has a sufficient NEDL for detecting concentration differences of CHL: based on the 1995 performance values AVIRIS can detect  $2.8 \text{ mg m}^{-3}$  CHL at concentration levels of  $20 \text{ mg m}^{-3}$  and  $22 \text{ mg m}^{-3}$  CHL at  $200 \text{ mg m}^{-3}$  CHL. Using smart algorithms these accuracies may even improve. Ofcourse in a real remote sensing mission these values will deteriorate due to the influence of the atmosphere and a rough water surface.

The parameters as they have been defined here are representative only for these lakes. E.g. the phytoplankton fraction of seston dry weight was calculated using the data from Buiteveld (1995). Other phytoplankton occurring in these lakes such as *Prochlorothrix hollandica* have a different ratio:  $DW = 0.048 \text{ CHL}$  (Rijkeboer et al. 1990). For samples of 12 lakes taken in May 1994 the value for phytoplankton equivalent dry weight fraction was  $DW = 0.059 \text{ CHL}$  (calculated from data in Gilijamse, 1994). This value is perhaps more realistic as it is representative for natural populations of algae.

The model presented here is part of a pilot study on the use of forward models (from the inherent optical water properties to remotely sensed radiance). The model needs to be tested more thoroughly with field and laboratory data. The input parameters may be improved and made more generally applicable. Foreseen developments are the inclusion of a realistic air/water interface including waveglint and whitecapping; as well the inclusion of an atmosphere model. It is also intended to use the forward model for developing inverse analytical methods for estimating water quality parameters from remotely sensed radiance data.

## 6. REFERENCES

- Buiteveld, H., 1995, A model for calculation of diffuse light attenuation (PAR) and secchi depth *Netherlands journal of aquatic ecology*, vol. 29, pp. 55-65, 1995.
- Buiteveld, H., J. H. M. Hakvoort, and M. Donze, 1995, Optical properties of pure water ed. J. S. Jaffe. XII, pp. 174-183, 1994. Ocean Optics XII. SPIE. Bellingham, Washington, USA.
- Dekker, A.G., 1993, Detection of optical water quality parameters for eutrophic waters by high resolution remote sensing, pp. 1-240
- Dekker, A.G. and M. Donze, 1994, Imaging spectrometry as a research tool for inland water resources analysis. In: ed. J.Hill. Dordrecht, The Netherlands: Kluwer AP.
- Dekker, A.G., H. J. Hoogenboom, L. M. Goddijn, and T. J. M. Malthus, 1994, The relationship between spectral reflectance, absorption and backscattering for four inland water types pp. 245-252, 1994. 6th Intern. Symp. on Physical Measurements and Signatures in Remote Sensing. CNES, France. Val d'Isere.
- Gilijamse, L.I., 1994, Absorption coefficients of phytoplankton and tripton in some Netherlands lakes; Student Report nr. 1994, Netherlands Institute for Ecological Research, Centre for Limnology, Royal Dutch Academy of Sciences, Nieuwersluis, The Netherlands. pp 1-53.
- Gordon, H. R., O. B. Brown, and M. M. Jacobs, 1975, Computed relationships between the inherent and apparent optical properties of a flat homogeneous ocean *Applied Optics*, vol. 14, pp. 417-427.
- Gordon, H. R. and A. Morel. *Remote assessment of ocean color for interpretation of satellite visible imagery: a review*, New York: Springer-Verlag, 1983. pp. 1-114.
- Jerlov, N.G., 1976, *Marine Optics*, Amsterdam, the Netherlands.
- Kirk, J. T. O., 1991, Volume scattering function, average cosines, and the underwater light field *Limnol. Oceanogr.* vol. 36, pp. 455-467.
- Kirk, J. T. O., 1994, *Light & photosynthesis in aquatic ecosystems*, pp. 1-509.
- Morel, A. and H. R. Gordon, 1980, Report of the working group on water color *Boundary-Layer Meteorology*. vol. 18, pp. 343-355.
- Morel, A. and L. Prieur, 1977, Analysis of variations in ocean colour *Limnol. Oceanogr.* vol. 22, pp. 709-722.
- Whitlock, C. H., L. R. Poole, J. Usry, W. M. Houghton, W. G. Witte, W. D. Morris, and E. A. Gurganus, 1981, Comparison of reflectance with backscatter and absorption parameters for turbid waters *Applied Optics*, vol. 20, pp. 517-522.